PLETHORA and WOX5 interaction and subnuclear localisation regulates *Arabidopsis* root stem cell maintenance

Rebecca C. Burkart[1], Vivien I. Strotmann[1], Gwendolyn K. Kirschner[1,2], Abdullah Akinci[1], Laura Czempik[1,3], Alexis Maizel[4], Stefanie Weidtkamp-Peters[5], Yvonne Stahl[1*]

[1]Institute for Developmental Genetics, Heinrich-Heine University, Universitätsstr. 1, 40225 Düsseldorf, Germany

[2]present affiliation: Institute for Crop Science and Resource Conservation, Crop Functional Genomics, University of Bonn, Friedrich-Ebert-Allee 144, 53113 Bonn, Germany

[3]present affiliation: Molecular Plant Science/Plant Biochemistry, University of Wuppertal, Gaußstraße 20, 42119 Wuppertal, Germany

[4]Center for Organismal Studies (COS), University of Heidelberg, Im Neuenheimer Feld 230, 69120 Heidelberg, Germany

[5]Center for Advanced Imaging, Heinrich-Heine University, Universitätsstr. 1, 40225 Düsseldorf, Germany

[*]Correspondence should be addressed to Y.S. (E-mail Yvonne.Stahl@hhu.de)

Key words: stem cells, root meristem, differentiation, transcription factor complexes, nuclear bodies, prion-like domains

Total word count: 7260

Abstract

Maintenance and homeostasis of the stem cell niche (SCN) in the *Arabidopsis* root is essential for growth and development of all root cell types. The SCN is organized around a quiescent center (QC) that maintains the stemness of the cells in direct contact. The transcription factors WUSCHEL-RELATED HOMEOBOX 5 (WOX5) and the PLETHORAs (PLTs) are both expressed in the SCN where they maintain the QC and regulate the fate of the distal columella stem cells (CSCs). Although WOX5 and PLTs are known as important players in SCN maintenance, much of the necessary regulation of quiescence and division in the *Arabidopsis* root is not understood on a molecular level. Here, we describe the concerted mutual regulation of the key transcription factors WOX5 and PLTs on a transcriptional and protein interaction level, leading to a confinement of the WOX5 expression domain to the QC cells by negative feedback regulation. Additionally, by applying a novel SCN staining method, we demonstrate that both WOX5 and PLTs are necessary for root meristem maintenance as they regulate QC quiescence and CSC fate and show that QC divisions and CSC differentiation correlate. Moreover, we uncover that PLTs, especially PLT3, contains intrinsically disordered prion-like domains (PrDs) that are necessary for complex formation with WOX5 and its recruitment to subnuclear microdomains/nuclear bodies (NBs) in the CSCs. We propose that the partitioning of the PLT-WOX5 complexes to NBs, possibly by liquid-liquid phase separation, plays an important role during determination of CSC fate.

Introduction

The root system of higher plants is essential for plant life, as it provides anchorage in the soil and access to nutrients and water. It arises from a population of long-lasting stem cells residing in a structure called root apical meristem (RAM) at the tip of the root. Within the *Arabidopsis thaliana* RAM, the stem cell niche (SCN) consists of on average four slowly dividing cells, the QC cells, which act as a long-term reservoir and signalling center by maintaining the surrounding shorter-lived, proliferating stem cells (also called initials) in a non-cell autonomous manner[1]. These stem cells continuously divide asymmetrically, thereby generating new stem cells that are still in contact with the QC. The hereby-produced daughter cells frequently undergo cell divisions and are shifted further away from the QC to finally differentiate. By this mechanism, the position of the stem cells in the root remains the same throughout development and their precise orientation of division leads to the formation of concentrically organized clonal cell lineages representing a spatio-temporal developmental gradient[1–3]. From the inside to the outside the following root cell layers develop: vasculature, pericycle, endodermis, cortex and epidermis plus columella and lateral root cap at the distal root tip (Fig. 1a).

The necessary longevity and continuous activity of the RAM can only be achieved if its stem cell pool is constantly replenished, since cells are frequently leaving the meristematic region due to continuous cell divisions. Therefore, complex regulatory mechanisms involving phytohormones and key transcription factors (TFs) regulate stem cell maintenance and the necessary supply of differentiating descendants[4]. Here, the APETALA2-type PLT TF family and the homeodomain TF WOX5 play important roles[5,6]. WOX5 is expressed mainly in the QC, but maintains the surrounding stem cells non-cell-autonomously by repressing their differentiation[6,7]. Loss of WOX5 causes the differentiation of the distal CSCs into starch-accumulating columella cells (CCs), while increased WOX5 expression causes CSC over-proliferation. Hence, WOX5 abundance is critical and necessary to suppress premature CSC

differentiation[6,7]. WOX5 also represses QC divisions, maintaining the quiescence of the QC by repressing CYCLIN D (CYCD) activity within the QC[8]. The auxin-induced PLTs form a clade of six TFs, and act as master regulators of root development, as multiple *plt* mutants fail to develop functional RAMs[5,9,10]. PLT1, 2, 3 and 4 are expressed mainly in and around the QC and form an instructive gradient, which is required for maintaining the balance of stem cell fate and differentiation. This PLT gradient is also necessary for separating auxin responses in the SCN and for the correct positioning of the QC and the expression of QC markers[5,9,10]. Genetically, WOX5 and PLT1 were shown to play an interconnected role in auxin-regulated CSC fate, whereas PLT1 and PLT3 were found to positively regulate WOX5 expression[11,12].

Although the implication of PLTs and WOX5 in controlling stem cell regulation and maintenance in the *Arabidopsis* RAM is well established and genetic evidence for cross regulation exists, the underlying molecular mechanisms remain largely elusive. Here, we show that the mutual regulation of expression, but also the ability of PLTs, especially PLT3, to recruit WOX5 to NBs in CSCs controls stem cell homeostasis in the *Arabidopsis* RAM. We propose a model in which the differential PLT/WOX5 complexes depending on subnuclear localisation regulate stem cell fate in the RAM, possibly by phase separation of PLT3 to NBs.

Results

WOX5 and PLTs are essential players in distal stem cell maintenance[5–7,9]. This, as well as their overlapping expression and protein localisation domains in the root SCN raised the question if they could act together in distal stem cell regulation, where, in comparison to all the other PLTs, particularly PLT3 is highly expressed (Fig. 1b)[9]. First, we tested if WOX5 influences *PLT3*-expression. Both a transcriptional and translational PLT3 fluorescent reporter line showed a reduced expression in the QC and CSC of a *wox5* mutant to around 60 % compared to the *Col-0* wild type roots (Fig. 1b-g, Suppl. Table 5). This extends the previously reported regulation of *PTL1* expression by WOX5[11] and shows that WOX5 positively regulates expression of several *PLTs*. To test if *WOX5* expression also depends on PLTs, we used a transcriptional reporter, which expresses a nuclear-localised mVenus from the *WOX5* promoter. In agreement with previous reports, expression of *WOX5* in our transcriptional reporter line is confined to the QC and is only weakly expressed in the stele initials[6,7] (Fig. 2a). In *plt2* and *plt3* single mutants, we observed additional mVenus-expressing cells in the QC region, which may derive from aberrant periclinal cell divisions in the QC (Fig. 2b,c, Suppl. Table 6). This effect is even stronger in the *plt2, plt3* double mutant roots, where extra cells are found in all observed roots and often even form an additional cell layer of *WOX5* expressing cells (Fig. 2d). We quantified the number of *WOX5* expressing cells and the area of *WOX5* expression per root by acquiring transverse optical sections through the roots. Previously, it was reported that the *Arabidopsis* wild type QC is composed of three to five cells with a low division rate[2,13–15]. Applying our method, we observed four to nine *WOX5* expressing cells in the *Col-0* wild type (Fig. 2e,g, Suppl. Table 6), whereas we found nine to 14 *WOX5* expressing cells and a laterally expanded *WOX5* expression domain in the *plt2, plt3* double mutants (Fig. 2f,g,h, Suppl. Table 6). Taken together, our data show that WOX5 positively regulates *PLT3* expression, whereas PLT2 and

105 PLT3 synergistically restrict *WOX5* to its defined expression domain in the QC, possibly by
106 negative feedback regulation.

107 QC cells rarely divide as they provide a long-term reservoir to maintain the surrounding stem
108 cells[13,16]. As WOX5 and PLTs control QC cell divisions and CSC maintenance[5–10], we asked if
109 these two aspects are interdependent. Therefore, we analysed the cell division rates in the QC
110 and the CSC phenotypes in wild type and mutant roots. To asses these two phenotypes and to
111 probe for their interdependency, we had to measure the number of dividing QC cells and CSC
112 layers within the same root simultaneously. Therefore, we established a novel staining method,
113 named SCN staining, by combining the 5-ethynyl-2'-deoxyuridine (EdU) and modified pseudo
114 Schiff base propidium iodide (mPS-PI) stainings to simultaneously visualise cell divisions,
115 starch granule distribution and cell walls within the same root[13,17]. Applying this new staining
116 combination, potential correlations between QC-divisions and CSC cell fates can be uncovered.
117 The EdU-staining provides a useful method to analyse QC-divisions by staining nuclei that
118 have gone through the S-phase, detecting cells directly before, during and after cell division[13].
119 However, cell layers and different cell types are hard to distinguish using only EdU staining
120 due to the lack of cell wall staining. Therefore, we used the mPS-PI-method to stain cell walls
121 and starch which is commonly used for CC and CSC cell fate characterisation[17–19]. CCs are
122 differentiated, starch granule-containing cells in the distal part of the root and mediate gravity
123 perception. They derive from the CSCs that form one or, directly after cell division, two cell
124 layers distal to the QC. The CSCs lack big starch granules and can thereby easily be
125 distinguished from the differentiated CCs by mPS-PI staining[17–19] (see Fig. 3a,b,i, raw data see
126 Suppl. Table 11).

127 WOX5 is necessary for CSC maintenance as loss of WOX5 causes their differentiation[6]. In
128 agreement with this, we found that the *wox5* mutants lack a starch-free cell layer in 78 % of
129 analysed roots, indicating differentiation of the CSCs, compared to 17% in *Col-0* (Fig. 3a,b,f,i,

Suppl. Table 7). In the *plt2* and *plt3* single mutants, the frequency of roots lacking a CSC layer increases to above 30 % (36 % and 32 %, respectively), and in the *plt2, plt3* double mutant to 41% (see Fig. 3c,d,e,i, Suppl. Table 7). Interestingly, the *wox5, plt3* double mutant as well as the *wox5, plt2, plt3* triple mutant show a frequency of differentiated CSCs comparable to the *wox5* single mutant (71 % and 77 %, respectively) (Fig. 3g,h,i, Suppl. Table 7). This data suggests that PLTs and WOX5 may act together in the same pathway to maintain CSC homeostasis, as there is no additive effect observable in the multiple mutant roots. To analyse QC division phenotypes in detail, we quantified the number of EdU-stained cells in QC position in transversal optical sections. In *Col-0*, 27 % of the analysed roots show at least one cell division in the QC within 24 hours (Fig. 3j,k,r, Suppl. Table 7), which is consistent with already published frequencies[13]. This frequency almost doubles to 45-50 % in the *plt2* and *plt3* single mutants and is even higher in the *plt2, plt3* double mutant (57 %) (Fig. 3l-n,r, Suppl. Table 7). Additionally, the *plt*-double mutant roots often show disordered QC regions with a disruption of the circular arrangement of cells surrounding the QC (Fig. 3n) which could be a result of uncontrolled divisions. In general, *wox5* mutants show a disordered SCN accompanied by a high overall QC cell division frequency of at least one dividing QC cell in 92 % of roots (Fig. 3o,r) and on average more dividing QC cells per root (Suppl. Table 7). The number of dividing QC cells per root increases further in the *wox5*, *plt3* double mutant and is even higher in the *wox5*, *plt2*, *plt3* triple mutant; here, in one third of the roots all QC cells undergo cell division (Fig. 3p-r, Suppl. Table 7). Taken together, this data suggest an additive effect of PLT2, PLT3 and WOX5 regarding the QC-division phenotype, in line with our hypothesis that WOX5 and PLTs act in parallel pathways to maintain the quiescence of the QC.

Additionally, we quantified roots showing at least one aberrant periclinal cell division in the QC in longitudinal optical sections (Suppl. Fig. 2). Whereas the occurrence of these aberrant periclinal divisions in *Col-0* wild type roots is very rare (3 %), it increases in the *plt*-single

mutants to 21 % and in *wox5* and *wox5, plt3* mutants to around 40 %. We found the most severe phenotypes in the *plt2, plt3* double and *wox5, plt2, plt3* triple mutants with an occurrence of periclinal QC-cell divisions in 53 % of the observed roots, indicating a predominant regulatory role of PLTs in periclinal QC cell divisions (Suppl. Fig. 2b, Suppl. Table 8).

To visualise correlations between QC division and CSC differentiation, we combined the acquired data in 2D-plots in which the frequencies of the two phenotypes are color-coded (Fig. 4). This visualisation reveals a regular pattern for *Col-0* wild type roots, which peaks at one CSC-layer and no QC-divisions (Fig. 4a). The pattern of the *plt* single mutants is more irregular with a shift to less CSC-layers (indicating more differentiation) and more EdU-stained QC cells (indicating more QC divisions) compared to the wild type *Col-0* roots (Fig. 4b,c). The *plt2, plt3* double mutants have an additional maximum at a position showing no CSC layer and one divided QC cell, resulting in two phenotypic populations, one at a wild type-like position, the other showing a strong mutant phenotype (Fig. 4d). The 2D-pattern for the *wox5* mutant shifts to less CSC-layers and more QC-divisions with a maximum at no CSC-layers and two QC-divisions (Fig. 4e). The QC phenotype is more severe in the *wox5, plt3* double mutant towards more cell divisions and is even stronger in the *wox5, plt2, plt3* triple mutant which peaks at zero CSC layers and three QC-divisions (Fig. 4f,g). In summary, our data suggests that higher CSC differentiation correlates with a higher division rate in the QC, possibly in order to replenish missing stem cells by increased QC divisions.

WOX5 and PLT3 are expressed and localise to overlapping domains in the SCN of the *Arabidopsis* root and based on our results regulate SCN maintenance together. To test for functionality of our reporter lines, we used the mVenus (mV) tagged WOX5 and PLT3 versions driven by their endogenous promoters for rescue experiments in the respective mutant phenotypes in *Arabidopsis.* We observed a full rescue of the *wox5* mutant expressing *pWOX5::WOX5-mV* and a partial rescue of the *plt3* mutant expressing *pPLT3::PLT3-mV*

indicating that the labelling with mVenus did not or only very little influence WOX5 or PLT3 functionality (Suppl. Fig. 1, Suppl. Table 14). In the PLT3-mV reporter line, we observed PLT3 localisation in bright subnuclear structures, hereafter called nuclear bodies (NBs). Most frequently, we found PLT3 NBs in young, developing lateral root primordia (LRP) (Fig. 5a, Suppl. Movie 1) already at stages where PLT1 and PLT2 are not yet expressed[20]. Importantly, we occasionally observed PLT3 NBs in CSCs of established main roots, but never in QC cells (Fig. 5b-c'). To further examine the PLT3 NBs in a context where no other PLTs are expressed, we used an estradiol-inducible system to control expression of PLT3 and WOX5 transiently in *Nicotiana benthamiana*[18]. Similar to our observations in *Arabidopsis*, we found that PLT3 mainly localises to NBs and to a lesser extend to the nucleoplasm (Fig. 6b). In co-expression experiments in *N. benthamiana*, we found that PLT3 recruits WOX5 to the same NBs, whereas on its own WOX5 remains homogenously localised within the nucleoplasm (Fig. 6g-g'', Suppl. Fig. 4a).

Next, we examined the domains possibly responsible for the localisation of PLT3 to NBs and found that the PLT3 amino acid (aa) sequence contains two glutamine (Q)-rich regions in the C-terminal part of the protein (see Fig. 6a). Proteins containing poly-Q stretches form aggregates or inclusions, a process often linked to pathological conditions in humans, such as Huntington's disease [21]. However, polyQ proteins also convey diverse cellular functions such as the promotion of nuclear assemblies (e.g. the transcription initiation complex), the formation of protein-protein complexes and the recruitment of other polyQ-containing proteins[22,23] as well as an enhancement in the transcriptional activation potential of TFs[22,24,25]. Interestingly, polyQs were also found to be enriched in TFs in plants[26]. Besides that, polyQ-containing proteins are proposed to act as key factors for the formation of RNA granules, which are ribonucleoprotein particles that mediate mRNA compartmentalisation[27]. Generally, the dynamic formation of subcellular structures could be necessary for a changing composition of the assemblies in

dependence of their functional status[23]. The transition of these proteins between condensed and soluble forms requires high flexibility in their protein structure, which is provided by the flexible polyQ-stretches. Poly-Q domains are predominantly positioned at the surface of a protein supporting the idea of their involvement in protein-protein interactions[28].

Next, we tested, if the polyQ-stretches in PLT3 are responsible for the subnuclear localisation and the recruitment of WOX5 to NBs. To this end, we deleted the polyQ domains of PLT3 and expressed the resulting PLT3ΔQ fused to mVenus transiently in *N. benthamiana*. We found that the subnuclear localisation and the recruitment of WOX did not change compared to the full-length PLT3 (see Fig. 6b,c,h-h''). Therefore, we conclude that the polyQ domain in PLT3 is not, or at least not alone, responsible for the subnuclear localisation and translocation to NBs.

Apart from proteins with polyQ domains, many proteins that form concentration-dependent aggregates contain larger, intrinsically disordered regions (IDRs) with a low complexity similar to yeast prions[29]. Recently, the existence of more than 500 proteins with prion-like behaviour in *Arabidopsis* was reported[30] and the presence of prion-like domains (PrDs) in protein sequences are predictable with web-based tools[31]. Therefore, we analysed the PLT and WOX5 sequences using the PLAAC PrD prediction tool and found that PLT3 has three predicted PrDs in its aa sequence, two of them located at the C-terminus, containing the two polyQ-stretches (see Fig. 6a, Suppl. Fig. 4). PLT1 and PLT2 also show two predicted PrD domains, each, but no polyQ stretches within them. WOX5 does not show any predicted PrD domains, nor any polyQ stretches (Suppl. Fig. 4). Just like polyQ-proteins, prions are responsible for some neurodegenerative diseases in mammals[33,34], but also their functional nature is becoming more eminent. The beneficial function of prions as a protein-based memory is highly discussed as their self-replicating conformations could act as molecular memories to transmit heritable information[32,36]. Prion-like proteins in *Arabidopsis* were first discovered by analysing protein sequences of 31 different organisms, identifying Q- and N-rich regions in the proteins to be

sufficient to cause protein aggregation[37]. In order to test the importance of the PrD domains in PLT3, we replaced the first PrD by a 27 aa linker (AAGAAGGAGGGAAAAAGGAGAAAAAGA) and deleted the C-terminally located PrDs. The resulting PLT3-version (PLT3ΔPrD) was fused to the mVenus FP and expressed in *N. benthamiana* epidermal cells. We did not observe a localisation of PLT3ΔPrD-mVenus to NBs, but in contrast a homogenous distribution within the nucleus (Fig. 6d). In addition, upon co-expression of PLT3ΔPrD-mVenus with WOX5-mCherry, we observed that WOX5 was no longer recruited to NBs (Fig. 6i-i''). In line with this, we observed PLT3 NBs in developing *Arabidopsis* LRP expressing pPLT3::PLT3-mVenus, but no more NBs were found in a pPLT3::PLT3ΔPrD-mVenus expressing line (Fig. 6e,f). Based on these observations, we conclude that the PrD domains of PLT3 are responsible for the localisation to NBs and the recruitment of WOX5 to NBs.

Proteins containing polyQ-stretches or PrDs are often involved in RNA binding, RNA processing and/or RNA compartmentalisation[27,35,38–41]. To test if PLT3 is involved in these processes, we performed an RNA-staining in *N. benthamiana* epidermal cells transiently expressing PLT3-mVenus with 5-ethynyl-2'-uridine (EU) (see Fig. 6j-j'''). EU is incorporated into RNA during transcription and we found that most of the stained RNA co-localises with the PLT3-mVenus NBs except for the EU-stained nucleolus (see Fig. 6j-j'''). Based on these observations, we conclude that the PLT NBs act as important sites for the recruitment of RNA and other factors, including WOX5.

Because the WOX5 and PLT protein expression domains overlap in the SCN and PLT1, PLT2 and PLT3 contain PrD domains, we asked whether PLTs and WOX5 interact *in vivo*, especially in light of the observed recruitment of WOX5 to PLT3 NBs. For this, we used fluorescence lifetime imaging microscopy (FLIM) to measure Förster resonance energy transfer (FRET) in order to analyse the potential protein-protein interaction of WOX5 and PLTs *in vivo*. To

perform FLIM, we inducibly co-expressed WOX5-mVenus as donor together with individual PLTs-mCherry as acceptors for FRET in *N. benthamiana* leaf epidermal cells. The fluorescence lifetime of the donor fluorophore mVenus fused to WOX5 alone is 3.03 ± 0.03 ns. A reduction of fluorescence lifetime is due to Förster resonance energy transfer (FRET) of the two fluorophores in very close proximity (≤ 10 nm) mediated by the interaction of the two observed proteins. When free mCherry is co-expressed as a negative control the WOX5-mVenus mean fluorescence lifetime is not significantly decreased (2.97 ± 0.07 ns) (Fig. 7a,b,h, Suppl. Table 12). When WOX5-mVenus is co-expressed with PLT1-mCherry the fluorescence lifetime significantly decreases to 2.8 ± 0.12 ns, with PLT2-mCherry to 2.7 ± 0.13 ns and with PLT3-mCherry to 2.7 ± 0.17 ns, indicating FRET and hence protein-protein interactions (Fig. 7c-e,h, Suppl. Table 12). The observed interaction of WOX5 with PLT1, PLT2 or PLT3 lead us to assume that they regulate SCN maintenance by the formation of complexes, either all together or in diverse compositions depending on the cell identity or their function. Interestingly, we observed a stronger lifetime decrease of WOX5-mVenus in the PLT3 NBs than in the nucleoplasm, indicating that the NBs function as main interaction sites of WOX5 with PLT3 (Fig. 7 i,j).

To address this, we measured the interaction between WOX5 and PLT3 in *Arabidopsis* roots via FLIM experiments in a translational line expressing WOX5-mVenus and PLT3-mCherry under control of their respective endogenous promoters. This results in very low protein concentration in comparison to the inducible system used in *N. benthamiana*. Probably due to this, we could not observe NBs in established root meristems of our *Arabidopsis* FLIM line and we could not measure a relevant decrease in fluorescence lifetime in contrast to the above-described experiments in *N. benthamiana* (Suppl. Fig. 3, Suppl. Table 13). In *Arabidopsis* seedlings, we only sometimes observed PLT3 NBs in the CSC layer of the root tip, but more

279 frequently in young, developing LRP (Fig. 5), whereas in *N. benthamiana* we observed NBs in
280 almost all cells. Therefore, we argue that the formation of the NBs is concentration dependent.

281 Moreover, we asked if the PrD and poly-Q domains in PLT3 are necessary for protein-protein
282 interaction with WOX5. To test this, we performed FLIM experiments with mCherry-tagged
283 full-length PLT3, PLT3ΔQ and PLT3ΔPrD as acceptors and WOX5-mVenus as donor in *N.*
284 *benthamiana*. Here, we observed that co-expression of the PLT3 deletion variants did not lead
285 to a significantly reduced fluorescence lifetime and therefore no protein-protein interaction
286 takes place in comparison to the full-length version (see Fig. 7e-h). This implies that PrD
287 domains containing the polyQ domains in PLT3 are necessary for the NB localisation, but also,
288 notably, for protein complex-formation with WOX5.

289 In summary, our findings show that QC quiescence and CSC maintenance are mediated by
290 mutual transcriptional regulation of PLTs and WOX5 as well as their direct protein-protein
291 interaction and subnuclear partitioning to NBs due to PrDs.

Discussion

Based on our results we propose that the regulation of QC quiescence and CSC maintenance is mediated by mutual transcriptional regulation of PLTs and WOX5 by a negative feedback loop. Here, a high *PLT* expression in the QC-region is promoted by WOX5, which again confines WOX5 to a defined and restricted number of QC cells. In line with this, loss of PLTs lead to an expanded expression domain of *WOX5* and a decreased QC quiescence as more QC divisions occur. These observations are in agreement with previous findings, although just a minor role for PLT1 and PLT2 in confining *WOX5* expression was previously reported, as 17 % of *plt1, plt2* double mutant roots showed *WOX5* expression expanding into endodermal and columella stem cells[6]. As *WOX5* expression is normally limited to the QC, the question arises if, in absence of PLTs, either the *WOX5* expression domain expands to regions surrounding the QC or the QC region itself expands and therefore also the expression domain of *WOX5*. Interestingly, previous analyses show that the expression of several QC markers is missing or highly reduced in *plt* mutants, suggesting that they fail to maintain an intact QC[5]. The higher frequency of cell divisions in the QC region of *wox5* mutants can be explained by the reduced expression of *PLTs,* which consequently negatively impacts QC quiescence but also by a PLT-independent pathway where WOX5 itself may have a positive function on the QC quiescence. Previous findings suggest that WOX5 maintains QC quiescence through the repression of CYCD activity[8]. In light of our observation that PLT2, PLT3 and WOX5 show additive effects regarding the QC division phenotype, we propose a model in which WOX5 and PLTs could act in parallel pathways to maintain QC quiescence. The observed correlation between reduced QC quiescence and higher CSC differentiation could be a measure to replenish missing stem cells by QC divisions. This possible explanation is in agreement with the proposed function of the QC to serve as long-term stem cell reservoir, especially in case of stress or damage[16]. Supporting this, previous studies showed, even though uncorrelated, that loss of PLTs lead to

317 CSC differentiation and also an increase in ectopic cell divisions in the QC[5,11]. For CSC
318 homeostasis, PLTs and WOX5 may act together in the same pathway, possibly by complex
319 formation, as there is no observable additive effect in the multiple mutant roots which is in
320 agreement with previous findings[11]. The potential of WOX5 to physically interact with PLT1,
321 PLT2 and PLT3 indicates that they regulate CSC maintenance by the formation of complexes,
322 either all together or in diverse homo- or heteromeric compositions depending on cell identity
323 or function. In transient *N. benthamiana* experiments, PLT3 forms NBs and recruits WOX5
324 into them. The stronger lifetime decrease in NBs compared to the nucleoplasm measured by
325 FLIM implies that the NBs function as sites for protein-protein interaction of WOX5 with
326 PLT3. We could observe PLT3 NBs in cells of the CSC layer of some *Arabidopsis* main root
327 tips, but never in the QC region. On the other hand, PLT3 NBs were found more frequently in
328 several cells of developing LRPs. LRPs are in a younger and less-determined stage than the
329 main root and the observed subnuclear localisation to NBs could represent a marker for the
330 occurring determination and future cell differentiation. This goes along with the observed
331 localisation of PLT3 to NBs in the CSCs in some of the main roots. The PLT3 NBs could
332 represent compartments for the recruitment of and interaction with WOX5 and possibly other
333 factors involved in CSC fate determination and maintenance. Furthermore, we found that PLT3,
334 in contrast to PLT1 and PLT2, has polyQ containing PrDs in its aa sequence that are necessary
335 for the localisation to NBs and for complex-formation with WOX5. Proteins containing polyQ-
336 stretches or PrDs are often involved in RNA binding, RNA processing and/or RNA
337 compartmentalisation[27,35,38–41] and indeed, the PLT3 NBs co-localise with RNA. Just as PLT3,
338 FLOWERING CONTROL LOCUS A (FCA) is a PrD-containing protein[30] that localises to
339 subnuclear structures[41]. The FCA bodies separate from the cytosol by liquid-liquid phase
340 separation to provide compartments for RNA 3'-end processing factors[41]. Similarly, PLT3 NBs
341 could represent compartments for the recruitment of interacting factors and RNA for further

342 processing, sequestration or transportation. As PLT3 is a TF, the co-localising RNA could also
343 represent newly transcribed RNA at the transcription sites where PLT3 binds to DNA, e.g. the
344 WOX5 promoter region[12]. The possible liquid-like nature of the PLT3 NBs will be an
345 interesting subject for further studies investigating its putative phase separation properties.

346 To summarize our results in a model, we propose that the regulation of QC quiescence and CSC
347 maintenance are not only mediated by the mutual transcriptional regulation of PLT and WOX5,
348 but also, importantly, by building protein complexes that are differentially localised within
349 distinct nuclei in the SCN (see Fig. 8). The observed subnuclear localisation of PLT3 to NBs
350 could represent a marker for the determination to future cell differentiation in the CSC layer.
351 Furthermore, the PrD and polyQ domains in PLT3 may act as an initial starting point to
352 compartmentalise and partition WOX5 that has moved from the QC towards the CSC layer into
353 RNA-containing nuclear bodies, possibly by concentration-dependent liquid-liquid phase
354 separation process. The observed sites could represent transcriptionally active sites for the
355 regulation of target genes involved in CSC fate determination. The dynamic
356 compartmentalization to subcellular or subnuclear microdomains of proteins with intrinsically
357 disorderd, PrD and/or polyQ domains was shown to have severe effects, e.g. in human
358 pathological disorders (e.g. Huntington's disease). In *Arabidopsis,* it could present a fast and
359 reversible concentration-dependent regulatory mechanism[29], e.g. in case of PLT3 and WOX5
360 to determine CSC cell fate. It remains to be determined if liquid-liquid phase separation is the
361 underlying mechanism of the observed subnuclear compartmentalisation and if also other
362 processes in determination of cell fates and stemness in *Arabidopsis* are regulated by this
363 mechanism.

Methods

Cloning. pWOX5::mVenus-NLS, pWOX5::WOX5-mVenus, pPLT3::PLT3-mVenus, pPLT3::PLT3-mCherry, pPLT3::PLT3ΔPrD-mVenus and β-estradiol inducible PLT3ΔPrD-mVenus were created by using the GreenGate cloning method [42]. The internal *BsaI* restriction sites in the WOX5 promoter and WOX5 CDS were removed by PCR amplification of the sequences upstream and downstream of the *BsaI* sites with primer pairs whereof one primer has an altered nucleotide sequence at this site (Supplementary Table 1), followed by an overlap extension PCR to reconnect the gene fragments. The sequences upstream of the ATG start codon of WOX5 (4654 bp) and PLT3 (4494 bp) were used as promoter regions and were amplified by PCR and primers to add flanking *BsaI* restriction sites and matching overlaps for the GreenGate cloning system. Afterwards they were cloned into the GreenGate entry vector pGGA000 via *BsaI* restriction and ligation. The GreenGate promoter module carrying the β-estradiol inducible cassette was provided by [43]. The CDS of WOX5, PLT3 and PLT3ΔPrD as well as the FPs mVenus and mCherry were amplified by PCR using adequate primer pairs to add flanking *BsaI* restriction sites and matching overlaps for cloning into the GreenGate entry vectors pGGC000 (for CDS) and pGGD000 (for FPs) via *BsaI* restriction and ligation. All created entry vectors were confirmed by sequencing. The expression cassettes were created with a GreenGate reaction using pGGZ001 as destination vector. The correct assembly of the modules was controlled by sequencing. All module combinations used to construct the expression vectors can be found in Supplementary Table 3.

All other inducible constructs for *N. benthamiana* expression (free mCherry, WOX5-mVenus, PLT1-mVenus, PLT2-mVenus, PLT3-mVenus, PLT3ΔQ-mVenus) were created by Gateway cloning (Invitrogen™, Thermo Fisher Scientific Inc.). The CDS of WOX5, PLT1, PLT2, PLT3 and PLT3ΔQ were amplified and cloned into pENTR/D-TOPO®. The Entry-vectors were confirmed by sequencing. The destination vector carrying the mVenus (pRD04) is based on

pMDC7 [44] which contains a β-estradiol inducible system for expression *in planta*. The mVenus was introduced via restriction/ligation C-terminally to the Gateway cloning site. The destination vector carrying the mCherry (pABindmCherry) was described before [45]. The expression vectors were created by LR-reaction of destination and entry vectors. Gateway expression vectors were verified by test digestion.

For the creation of the domain-deletion variants of PLT3 (PLT3ΔQ and PLT3ΔPrD), the CDS parts upstream and downstream of the desired sequence deletions were amplified with PCR and afterwards reconnected with overlap-PCR. The 27 aa linker (AAGAAGGAGGGAAAAAGGAGAAAAAGA) to replace the first PrD in PLT3ΔPrD was also introduced by overlap-PCR. All primer used for cloning can be found in Supplementary table 1.

plant work. All *Arabidopsis* lines used in this study were in the Columbia (*Col-0*) background. The single mutants *wox5-1* and *plt3-1* have been described before[9] (Supplementary table 4). The *plt2* (SALK_128164) and *wox5-1* (SALK038262) single mutants were provided by the *Arabidopsis* Biological Resource Center (ABRC, USA). The homozygous double and triple mutants were created by crossings (Supplementary table 4) and homozygous F3 genotypes were confirmed by PCR with appropriate primer pairs (Supplementary Table 2). The transgenic lines were created by floral dip as described before[46] except for the published, transgenic *Col-0* lines with pPLT3::erCFP and pPLT3::PLT3-YFP[9] constructs.They were crossed into the *wox5-1* mutant background. Homozygous lines were confirmed by genotyping and hygromycin selection. All plants for crossing, floral dips, genotyping and seed amplification were grown on soil in phytochambers under long day (16 h light/ 8 h dark) conditions at 21 °C. For microscopy *Arabidopsis* seeds were fume-sterilised (50 ml 13 % sodiumhypochlorite (v/v) + 1 ml hydrochloric acid), imbedded in 0.2 % (w/v) agarose, stratified at 4 °C for 2 days and plated on GM agar plates (1/2 strength Murashige Skoog medium including Gamborg B5 vitamins, 1.2 %

(w/v) plant agar, 1 % (w/v) sucrose, supplemented with 0.05 % (w/v) MES hydrate). *Arabidopsis* seedlings were grown for 5 days under continuous light at 21 °C and directly imaged afterwards.

Cell wall and plasma membrane staining. For root imaging, the cell walls in *Arabidopsis* seedlings were stained by incubation in aqueous solutions of either 10 µM propidium iodide (PI) or 2.5 µM FM4-64 dye (Invitrogen™, Thermo Fisher Scientific Inc.). The staining solution was used as mounting medium for microscopy.

***N. benthamiana* infiltration.** For transient gene expression in *N. benthamiana*, the *Agrobacterium* strain GV3101::pMP50 was used as vector, carrying plasmids with the desired constructs and additionally either the helper plasmid p19 as silencing suppressor or the helper plasmid pSOUP that harbours a replicase needed for GreenGate vectors. Cultures were grown over night in 5 ml dYT-medium at 28 °C on a shaker. The cultures were centrifuged for 10 min at 3345 g, the pellet was resuspended in infiltration medium (5 % (w/v) sucrose, 0.01 % (v/v) Silwet, 0.01 % (w/v) MgSO4, 0.01 % (w/v) glucose, 450 µM acetosyringone) to an optical density OD_{600} of 0.4 and cultures were incubated for one hour at 4 °C. The infiltration was done either with one single or with a combination of two different *Agrobacteria* cultures for co-expression of two constructs. A syringe without needle was used for the infiltration on the adaxial side of the leaves of well-watered *N. benthamiana* plants. For the expression of GreenGate constructs, an *Agrobacterium* strain carrying the p19 plasmid was co-infiltrated. The expression was induced 2-5 days after infiltration by applying an aqueous β-estradiol solution (20 µM β-Estradiol, 0.1 % (v/v) Tween®-20) to the adaxial leaf surface. Imaging or FLIM experiments were done 3 to 16 hours after induction, depending on the expression level.

SCN staining. *Arabidopsis* seedlings were grown under continuous light for 5 days on GM agar plates without sucrose and then transferred on fresh plates containing additionally 7 µg/ml EdU to continue growing for 24 hours. Afterwards we performed an mPS-PI staining like

described before[17]. Preliminary to the clearing step, the EdU-staining was performed. The permeabilisation of the cells and the subsequent staining of EdU-containing DNA with Alexa Fluor® 488 was done as described in the Click-it® EdU Imaging Kits from Invitrogen™ (Thermo Fisher Scientific Inc.) with adapted incubation times for *Arabidopsis* seedlings (permeabilisation for 1-2 h and click-reaction for 1 h). The click-reaction cocktail was prepared freshly with self-made solutions (Tris buffer with 50 mM Tris and 150 mM NaCl at pH 7.2-7.5; 4 mM CuSO4; 1.5 µM Alexa Fluor® 488 picolyl azide; 50 mM ascorbic acid). The Alexa Fluor® 488 picolyl azide (Thermo Fisher Scientific Inc.) was added from a 500 µM stock in DMSO. The ascorbic acid was added last from a freshly prepared aqueous 500 mM stock solution. After staining was done, the clearing step with chloralhydrate was performed like described before[17].

Images were acquired with a ZEISS LSM880 confocal microscope. z-stacks through the QC-region were recorded to obtain transversal views. In order to calculate the CSC phenotype, the number of CSC layers was counted in xy-images of each root. The QC-division phenotype is the number of EdU-Alexa Fluor® 488-stained cells in the QC, which was counted in the cross-sectional images up to a maximal number of 4 stained QC cells. The phenotype frequencies of CSC differentiation and QC divisions (Fig. 3) where visualised in bar graphs with Excel (Microsoft Office 365 ProPlus, Microsoft Corporation). In order to correlate the two investigated phenotypes, we combined the CSC data and the QC-division data in 2D-plots. The combined QC/CSC-phenotype of every root was entered in a matrix with QC-divisions on the x- and CSC layers on the y-axis. 2D plots were created with Origin 2018b (OriginLab Corporation).

RNA staining. The RNA-staining in *N. benthamiana* epidermal cells was done on *N. benthamiana* leaves harboring a construct for a β-Estradiol inducible *PLT3-mVenus* expression. 5-ethynyl-2'-uridine (EU) was infiltrated in *N. benthamiana* leaves the day before staining. The

464 expression of PLT3-mVenus was induced the next morning, 3 hours before fixation of the plant
465 tissue. For fixation and permeabilisation of cells, pieces of the leaves were cut and treated with
466 4 % (w/v) paraformaldehyde and 0.5 % (v/v) TritonX-100 in PBS under vacuum for 1 h. The
467 click-reaction of EU with Alexa Fluor® 555 picolyl azide was performed similarly to the EdU-
468 Alexa Fluor® 488-staining described for the SCN staining in this article. A DAPI-
469 counterstaining was carried out afterwards by incubating the leaf pieces in 0.1 µg/ml DAPI for
470 30 min. PBS was used as mounting medium for imaging.

471 **Microscopy.** Imaging of *Arabidopsis* roots and *Nicotiana* leaves was carried out with a ZEISS
472 LSM780 or LSM880. Excitation and detection of fluorescent emission of fluorescent dyes was
473 done as follows: DAPI was exited at 405 nm and emission was detected at 408-486 nm,
474 Cerulean was excited at 458 nm and emission was detected at 460-510 nm; CFP was excited at
475 458 nm and emission was detected at 463-547 nm. mVenus was excited at 514 nm and emission
476 was detected at 517-560 nm, or for co-expression with red dyes excited at 488 nm and detected
477 at 500-560 nm. YFP was excited at 514 nm and emission was detected at 518-548 nm. Alexa
478 Fluor® 488 was excited at 488 nm and emission was detected at 490-560 nm. Alexa Fluor® 555
479 was excited at 561 nm and emission was detected at 565-640 nm. PI was excited at 561 nm and
480 emission was detected at 590-710 nm. FM4-64 was excited at 514 nm or 561 nm and emission
481 was detected at 670-760 nm. mCherry was excited at 561 nm and emission was detected at
482 590-640 nm. Imaging of more than one fluorophore was done in sequential mode to avoid cross
483 talk. The movie of pPLT3::PLT3-mVenus in a lateral root primordium was acquired with a
484 MuViSPIM (Luxendo, Bruker) light sheet microscope and a 40x/0.8 Nikon objective with a
485 1.5x tube lens on the detection axis to provide a 60x magnification.

486 **Image deconvolution.** The microscope images in Fig. 5 a, c-c' were deconvolved with
487 Huygens 16.10.0p3 64b (Scientific Volume Imaging B.V.).

488 **Analyses of expression patterns and levels in *Arabidopsis*.** For the comparison of relative
489 fluorescence levels in the SCN of 5 day old *Arabidopsis* seedlings expressing either
490 transcriptionally FP tagged *PLT3* (*pPLT3::erCFP*) or translationally FP tagged *PLT3*
491 (*pPLT3::PLT3-YFP*) driven by the endogenous PLT3 promoter in either the *Col-0* wild type or
492 the *wox5-1* mutant, images of 9-16 roots per genotype were acquired with constant settings per
493 FP. A ZEISS LSM880 confocal microscope was used. The mean fluorescence levels were
494 measured with Fiji[47] in equally sized rectangular ROIs including the QC and CSC positions in
495 the SCN. The thereby generated values were normalised to the *Col-0* mean fluorescence
496 intensity and visualised in box and scatter plots created with Origin 2018b (OriginLab
497 Corporation).

498 Images of the root tips of 5 day old *Arabidopsis* seedlings expressing *mVenus-NLS* driven by
499 the endogenous WOX5 promoter in *Col-0* and *plt2* or *plt3-1* single mutants and the *plt2,plt3*
500 double mutant were acquired. Additionally, z-stacks through the QC region of the roots were
501 recorded to get a transversal view of the QC. The visualisation and counting of nuclei with
502 *WOX5* expression (fig. 2) was done with Imaris (version 9.1.2, Bitplane, Oxford Instruments
503 plc). Box and scatter plots showing the number of expressing nuclei were created with Origin
504 2018b (OriginLab Corporation). For the heat-map images, 10 acquired images were overlaid
505 with Fiji[47] and the resulting fluorescence distribution was displayed with a 16-colors lookup
506 table. To calculate the area of lateral *WOX5* expression in the QC region, a freehand-ROI
507 surrounding the expressing cells was created in every image with Fiji[47]. The ROI-areas were
508 visualised in box and scatter plots created with Origin 2018b (OriginLab Corporation).

509 **FLIM measurements.** FLIM was performed either in *N. benthamiana* leaf epidermal cells
510 expressing the desired gene combinations or in roots of 6-10 dag old *Arabidopsis* seedlings
511 expressing *WOX5-mVenus* and *PLT3-mCherry* with their endogenous promoters. The FLIM
512 measurements in *Arabidopsis* were performed in LRPs due to higher fluorescence levels and

513 less movement during measurements compared to the RAM. mVenus-tagged proteins were
514 always used as donor and mCherry-tagged proteins as acceptor for FRET. A ZEISS LSM 780
515 was used for the experiments equipped with a single-photon counting device (Hydra Harp 400,
516 PicoQuant GmbH). The mVenus donor was excited with a linearly polarized diode laser (LDH-
517 D-C-485) at 485 nm and a pulse frequency of 32 MHz. The excitation power was adjusted to
518 0.1-0.5 µW at the objective (C-Apochromat 40x/1.2 W Corr M27, ZEISS) for experiments in
519 *N. benthamiana* and 1.5-2 µW for experiments in *Arabidopsis*. The higher laser power in
520 *Arabidopsis* was needed due to lower fluorescence levels. τ-SPAD single photon counting
521 modules with 2 channel detection units (PicoQuant GmbH) and a bandpass filter (534/39) were
522 used to detect parallel and perpendicular polarized emission of the mVenus fluorescence.
523 Images were acquired with a frame size of 256x256 pixel, a pixel dwell time of 12.6 µs and a
524 zoom factor of 8. 40 to 60 frames were recorded in the *N. benthamiana* experiments, 80 frames
525 in the experiments performed in *Arabidopsis*.

526 Fluorescent lifetimes were obtained by further analyses of the acquired data with
527 SymPhoTime64 (PicoQuant GmbH). The instrument response function (IRF) of the microscope
528 hardware is needed for fluorescence lifetime calculation to correct the system-specific internal
529 time lag between laser pulse and data acquisition. The IRF was recorded preliminary to each
530 experiment by time-correlated single photon counting (TCSPC) of an aqueous solution of
531 erythrosine B in saturated potassium iodide. For data analysis of *N. benthamiana* experiments,
532 an intensity threshold of 100-200 photons per pixel was applied to remove background
533 fluorescence and a monoexponential fit was used. Due to low fluorescence intensities in
534 *Arabidopsis* experiments, no threshold was applied to obtain the maximal possible photon
535 number. In this case, a two-exponential fit was used to separate the mVenus fluorescence signal
536 from the background fluorescence created by the plant tissue. This results in two lifetimes
537 whereof one matches with the mVenus fluorescence lifetime of about 3 ns and the other

representing the very short background lifetime of less than 0.4 ns. All data was obtained in at least two independent experiments. For visualisation of the lifetimes, box and scatter plots were created with Origin 2018b (OriginLab Corporation). Lifetime images of representative measurements were created with a pixel wise FLIM-fit in SymPhoTime64 (PicoQuant GmbH). The line graph showing the lifetime difference between the bodies and the nucleoplasm of WOX5-mVenus co-expressed with PLT3-mCherry was created using Excel (Microsoft Office 365 ProPlus, Microsoft Corporation).

Prediction of protein domains. The PrDs in the WOX5, PLT1, PLT2 and PLT3 aa sequences were predicted with the PLAAC application[31]. The nuclear localisation signals (NLSs) of WOX5 and the studied PLT proteins were predicted with cNLS Mapper[48] for WOX5 and PLT3 and SeqNLS[49] for PLT1 and PLT2.

Figure assembly. All figures in this study were assembled using Adobe Photoshop CS5 (Adobe Inc.).

Acknowledgements

We would like to acknowledge funding of R.C.B. by the Deutsche Forschungsgemeinschaft (DFG) through grant Sta1212/1-1 to Y.S. We thank Andrea Bleckmann for sharing the Greengate Cerulean construct, Renze Heidstra and Ben Scheres for sharing published *Arabidopsis* lines (PLT::PLT-YFP, PLT::CFP and *plt* mutants). We also thank Rüdiger Simon and Peter Welters for critical discussion.

Author contributions

R.C.B., V.I.S., A.A., L.C., and G.K.K. carried out the experiments. Y.S. and R.C.B. designed the experiments, analysed and interpreted the data. S.W.P. contributed to FLIM data analyses. A.M. carried out light sheet imaging. Y.S. and R.C.B. wrote the manuscript. All authors commented on the manuscript.

Competing interests

The authors declare no competing interests.

Material & correspondence

Correspondence and material requests should be addressed to Yvonne Stahl (Yvonne.Stahl@hhu.de).

References

1. van den Berg, C., Willemsen, V., Henriks, G., Weisbeek, P. & Scheres, B. Short-range control of cell differentiation in the Arabidopsis root meristem. *Nature* **390,** 287–289 (1997).
2. Dolan, L. *et al.* Cellular organisation of the Arabidopsis thaliana root. *Development* **119,** 71–84 (1993).
3. Benfey, P. N. & Scheres, B. Root development. *Curr Biol* **10,** 13 (2000).
4. Drisch, R. C. & Stahl, Y. Function and regulation of transcription factors involved in root apical meristem and stem cell maintenance. *Front Plant Sci* **6,** 505; 10.3389/fpls.2015.00505 (2015).
5. Aida, M. *et al.* The PLETHORA genes mediate patterning of the Arabidopsis root stem cell niche. *Cell* **119,** 109–120; 10.1016/j.cell.2004.09.018 (2004).
6. Sarkar, A. K. *et al.* Conserved factors regulate signalling in Arabidopsis thaliana shoot and root stem cell organizers. *Nature* **446,** 811–814; 10.1038/nature05703 (2007).
7. Pi, L. *et al.* Organizer-Derived WOX5 Signal Maintains Root Columella Stem Cells through Chromatin-Mediated Repression of CDF4 Expression. *Dev Cell* **33,** 576–588; 10.1016/j.devcel.2015.04.024 (2015).
8. Forzani, C. *et al.* WOX5 suppresses CYCLIN D activity to establish quiescence at the center of the root stem cell niche. *Curr Biol* **24,** 1939–1944; 10.1016/j.cub.2014.07.019 (2014).
9. Galinha, C. *et al.* PLETHORA proteins as dose-dependent master regulators of Arabidopsis root development. *Nature* **449,** 1053–1057; 10.1038/nature06206 (2007).
10. Mähönen, A. P. *et al.* PLETHORA gradient formation mechanism separates auxin responses. *Nature* **515,** 125–129; 10.1038/nature13663 (2014).
11. Ding, Z. & Friml, J. Auxin regulates distal stem cell differentiation in Arabidopsis roots. *PNAS* **107,** 12046–12051; 10.1073/pnas.1000672107 (2010).
12. Shimotohno, A., Heidstra, R., Blilou, I. & Scheres, B. Root stem cell niche organizer specification by molecular convergence of PLETHORA and SCARECROW transcription factor modules. *Genes Dev* **32,** 1085–1100; 10.1101/gad.314096.118 (2018).
13. Cruz-Ramírez, A. *et al.* A SCARECROW-RETINOBLASTOMA protein network controls protective quiescence in the Arabidopsis root stem cell organizer. *PLoS biology* **11,** e1001724; 10.1371/journal.pbio.1001724 (2013).
14. Kidner, C., Sundaresan, V., Roberts, K. & Dolan, L. Clonal analysis of the Arabidopsis root confirms that position, not lineage, determines cell fate. *Planta* **211,** 191–199; 10.1007/s004250000284 (2000).
15. González-García, M.-P. *et al.* Brassinosteroids control meristem size by promoting cell cycle progression in Arabidopsis roots. *Development* **138,** 849–859; 10.1242/dev.057331 (2011).
16. Vilarrasa-Blasi, J. *et al.* Regulation of plant stem cell quiescence by a brassinosteroid signaling module. *Dev Cell* **30,** 36–47; 10.1016/j.devcel.2014.05.020 (2014).
17. Truernit, E. *et al.* High-resolution whole-mount imaging of three-dimensional tissue organization and gene expression enables the study of Phloem development and structure in Arabidopsis. *Plant Cell* **20,** 1494–1503; 10.1105/tpc.107.056069 (2008).

18. Stahl, Y. *et al.* Moderation of Arabidopsis root stemness by CLAVATA1 and ARABIDOPSIS CRINKLY4 receptor kinase complexes. *Curr Biol* **23,** 362–371; 10.1016/j.cub.2013.01.045 (2013).

19. Stahl, Y., Wink, R. H., Ingram, G. C. & Simon, R. A Signaling Module Controlling the Stem Cell Niche in Arabidopsis Root Meristems. *Curr Biol* **19,** 909–914; 10.1016/j.cub.2009.03.060 (2009).

20. Du, Y. & Scheres, B. PLETHORA transcription factors orchestrate de novo organ patterning during Arabidopsis lateral root outgrowth. *PNAS* **114,** 11709–11714; 10.1073/pnas.1714410114 (2017).

21. Scarafone, N. *et al.* Amyloid-like fibril formation by polyQ proteins: a critical balance between the polyQ length and the constraints imposed by the host protein. *PloS one* **7,** e31253; 10.1371/journal.pone.0031253 (2012).

22. Atanesyan, L., Günther, V., Dichtl, B., Georgiev, O. & Schaffner, W. Polyglutamine tracts as modulators of transcriptional activation from yeast to mammals. *Biol Chem* **393,** 63–70; 10.1515/BC-2011-252 (2012).

23. Mikecz, A. von. PolyQ fibrillation in the cell nucleus: who's bad? *Trends Cell Biol* **19,** 685–691; 10.1016/j.tcb.2009.09.001 (2009).

24. Schwechheimer, C., Smith, C. & Bevan, M. W. The activities of acidic and glutamine-rich transcriptional activation domains in plant cells: design of modular transcription factors for high-level expression. *Plant Mol Biol* **36,** 195–204 (1998).

25. Gerber, H. *et al.* Transcriptional activation modulated by homopolymeric glutamine and proline stretches. *Science* **263,** 808–811; 10.1126/science.8303297 (1994).

26. Kottenhagen, N., Gramzow, L., Horn, F., Pohl, M. & Theißen, G. Polyglutamine and Polyalanine Tracts Are Enriched in Transcription Factors of Plants. *German conference on Bioinformatics*; 10.4230/OASICS.GCB.2012.93 (2012).

27. Castilla-Llorente, V. & Ramos, A. PolyQ-mediated regulation of mRNA granules assembly. *Biochem Soc Trans* **42,** 1246–1250; 10.1042/BST20140099 (2014).

28. Totzeck, F., Andrade-Navarro, M. A. & Mier, P. The Protein Structure Context of PolyQ Regions. *PloS one* **12,** e0170801; 10.1371/journal.pone.0170801 (2017).

29. Cuevas-Velazquez, C. L. & Dinneny, J. R. Organization out of disorder: liquid-liquid phase separation in plants. *Curr Opin Plant Biol* **45,** 68–74; 10.1016/j.pbi.2018.05.005 (2018).

30. Chakrabortee, S. *et al.* Luminidependens (LD) is an Arabidopsis protein with prion behavior. *PNAS* **113,** 6065–6070; 10.1073/pnas.1604478113 (2016).

31. Lancaster, A. K., Nutter-Upham, A., Lindquist, S. & King, O. D. PLAAC: a web and command-line application to identify proteins with prion-like amino acid composition. *Bioinformatics (Oxford, England)* **30,** 2501–2502; 10.1093/bioinformatics/btu310 (2014).

32. Shorter, J. & Lindquist, S. Prions as adaptive conduits of memory and inheritance. *Nature reviews. Genetics* **6,** 435–450; 10.1038/nrg1616 (2005).

33. Aguzzi, A., Nuvolone, M. & Zhu, C. The immunobiology of prion diseases. *Nat. Rev. Immunol.* **13,** 888–902; 10.1038/nri3553 (2013).

34. Kim, H. J. *et al.* Mutations in prion-like domains in hnRNPA2B1 and hnRNPA1 cause multisystem proteinopathy and ALS. *Nature* **495,** 467–473; 10.1038/nature11922 (2013).

651 35. Alberti, S., Halfmann, R., King, O., Kapila, A. & Lindquist, S. A systematic survey
652 identifies prions and illuminates sequence features of prionogenic proteins. *Cell* **137,** 146–
653 158; 10.1016/j.cell.2009.02.044 (2009).

654 36. Bailey, C. H., Kandel, E. R. & Si, K. The persistence of long-term memory: a molecular
655 approach to self-sustaining changes in learning-induced synaptic growth. *Neuron* **44,** 49–
656 57; 10.1016/j.neuron.2004.09.017 (2004).

657 37. Michelitsch, M. D. & Weissman, J. S. A census of glutamine/asparagine-rich regions:
658 implications for their conserved function and the prediction of novel prions. *PNAS* **97,**
659 11910–11915; 10.1073/pnas.97.22.11910 (2000).

660 38. Schomburg, F. M., Patton, D. A., Meinke, D. W. & Amasino, R. M. FPA, a gene involved
661 in floral induction in Arabidopsis, encodes a protein containing RNA-recognition motifs.
662 *Plant Cell* **13,** 1427–1436 (2001).

663 39. Macknight, R. *et al.* FCA, a Gene Controlling Flowering Time in Arabidopsis, Encodes a
664 Protein Containing RNA-Binding Domains. *Cell* **89,** 737–745; 10.1016/S0092-
665 8674(00)80256-1 (1997).

666 40. Sonmez, C. *et al.* RNA 3' processing functions of Arabidopsis FCA and FPA limit intergenic
667 transcription. *PNAS* **108,** 8508–8513; 10.1073/pnas.1105334108 (2011).

668 41. Fang, X. *et al.* Arabidopsis FLL2 promotes liquid-liquid phase separation of
669 polyadenylation complexes. *Nature* **569,** 265–269; 10.1038/s41586-019-1165-8 (2019).

670 42. Lampropoulos, A. *et al.* GreenGate---a novel, versatile, and efficient cloning system for
671 plant transgenesis. *PloS one* **8,** e83043; 10.1371/journal.pone.0083043 (2013).

672 43. Denninger, P. *et al.* Distinct RopGEFs Successively Drive Polarization and Outgrowth of
673 Root Hairs. *Curr. Biol.* **29,** 1854-1865.e5; 10.1016/j.cub.2019.04.059 (2019).

674 44. Curtis, M. D. & Grossniklaus, U. A gateway cloning vector set for high-throughput
675 functional analysis of genes in planta. *Plant Physiol.* **133,** 462–469; 10.1104/pp.103.027979
676 (2003).

677 45. Bleckmann, A., Weidtkamp-Peters, S., Seidel, C. A. M. & Simon, R. Stem cell signaling in
678 Arabidopsis requires CRN to localize CLV2 to the plasma membrane. *Plant Physiol.* **152,**
679 166–176; 10.1104/pp.109.149930 (2010).

680 46. Zhang, X., Henriques, R., Lin, S.-S., Niu, Q.-W. & Chua, N.-H. Agrobacterium-mediated
681 transformation of Arabidopsis thaliana using the floral dip method. *Nat. Protoc.* **1,** 641–
682 646; 10.1038/nprot.2006.97 (2006).

683 47. Schindelin, J. *et al.* Fiji: an open-source platform for biological-image analysis. *Nat.*
684 *Methods* **9,** 676–682; 10.1038/nmeth.2019 (2012).

685 48. Kosugi, S., Hasebe, M., Tomita, M. & Yanagawa, H. Systematic identification of cell cycle-
686 dependent yeast nucleocytoplasmic shuttling proteins by prediction of composite motifs.
687 *PNAS* **106,** 10171–10176; 10.1073/pnas.0900604106 (2009).

688 49. Lin, J.-R. & Hu, J. SeqNLS: nuclear localization signal prediction based on frequent pattern
689 mining and linear motif scoring. *PloS one* **8,** e76864; 10.1371/journal.pone.0076864 (2013).

690

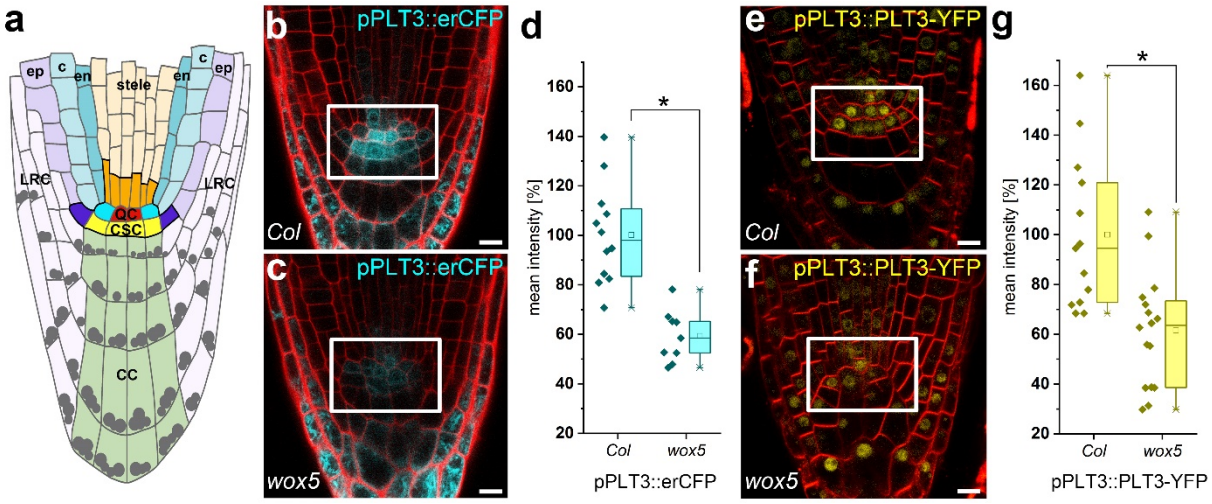

691

692 **Fig. 1 | WOX5 positively regulates PLT3 expression**. **a**, Schematic representation of the
693 *Arabidopsis* root meristem. The QC cells (red) maintain the surrounding stem cells (initials)
694 outlined in black together building the root stem cell niche (SCN). The different cell types are
695 colour-coded. QC = quiescent center (red); CSC = columella stem cells (yellow); CC =
696 columella cells (green); LRC = lateral root cap (light purple); ep = epidermis (dark purple); c =
697 cortex (light blue); en = endodermis (dark blue); **b**,**c**, Representative images of pPLT3::erCFP
698 (cyan) expressing and PI-stained (red) *Arabidopsis* roots in *Col* or *wox5* background,
699 respectively. **d**, Mean fluorescence intensities of the pPLT3::erCFP roots summarized in box
700 and scatter plots. The mean fluorescence intensity of the CFP signal in *Col* roots was to set to
701 100 %. **e**,**f**, Representative images of pPLT3::PLT3-YFP (yellow) expressing and FM4-64-
702 stained (red) *Arabidopsis* roots in *Col* or *wox5* background, respectively. **g**, Mean fluorescence
703 intensities of the pPLT3::PLT3-YFP expressing roots summarized in box and scatter plots. The
704 mean fluorescence intensity of the YFP signal in *Col* roots was to set to 100%. **d**,**g**, Box = 25-
705 75 % of percentile, whisker = 1.5 interquartile range, – = median, □ = mean value, × =
706 minimum/maximum. Asterisks indicate statistically significant differences as analyzed by one-
707 way ANOVA and post-hoc multiple comparisons using the Holm-Sidak test ($\alpha = 0.01$), number
708 of analyzed roots n = 9-16. **b**,**c**,**e**,**f**, Scale bars represent 10 µm. SCN = stem cell niche; PI =
709 propidium iodide; YFP = yellow fluorescent protein; CFP = cyan fluorescent protein.

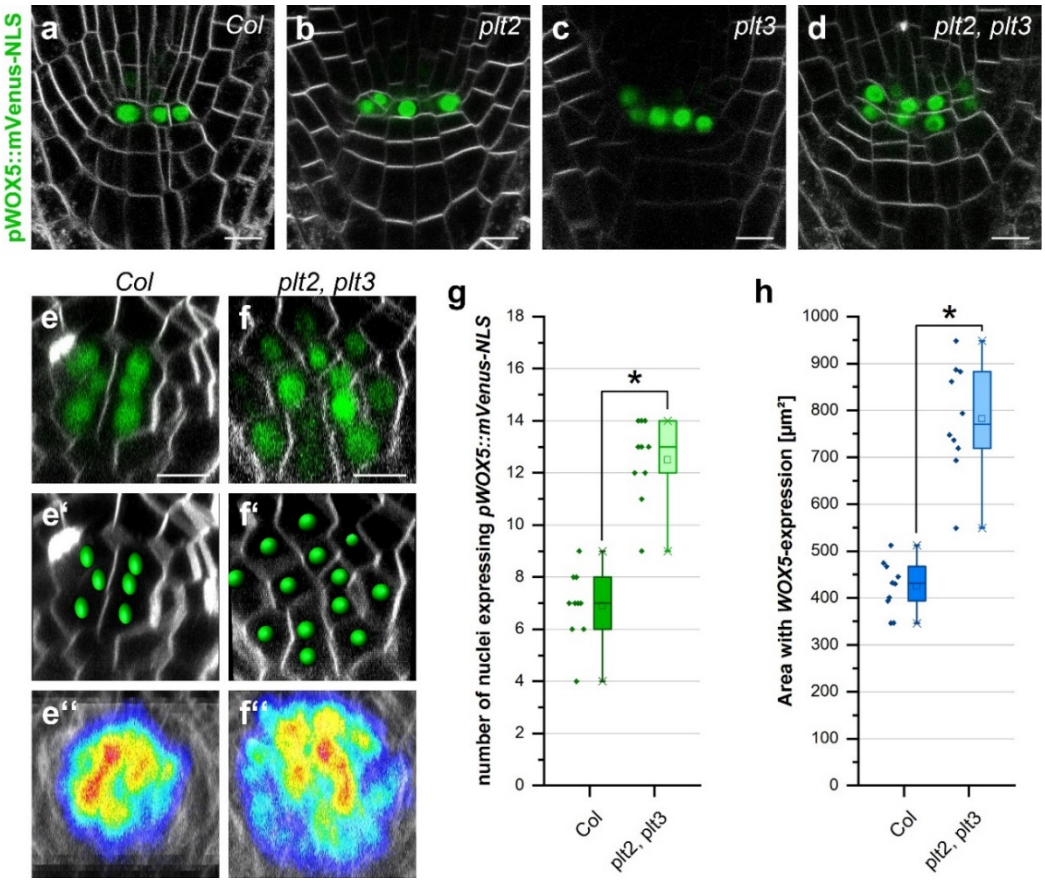

Fig. 2 | PLTs constrain the WOX5 expression domain. a-f, Representative FM4-64-stained *Arabidopsis* roots (grey) expressing pWOX5::mVenus-NLS (green) in *Col*, *plt2*, *plt3* and *plt2,plt3* double mutant background in longitudinal (**a-d)**, or transversal (**e-f**) optical sections. **e'**,**f'**, Analysis of representative images in (**e**) and (**f**) in Imaris in order to detect and count individual expressing nuclei. **e''**,**f''**, Overlay of 10 roots showing the area of detected fluorescence (high levels in red, low levels in blue) in *Col* and *plt2,plt3* double mutant roots. **g**, Number of nuclei expressing pWOX5::mVenus-NLS in *Col* and *plt2,plt3* double mutant roots summarized in box and scatter plots. **h**, Area of WOX5 expression in µm^2 in *Col* and *plt2,plt3* double mutant roots summarized in box and scatter plots. **g,h** Box = 25-75 % of percentile, whisker = 1.5 interquartile range, – = median, □ = mean value, × = minimum/maximum. Asterisks indicate statistically significant differences as analyzed by one-way ANOVA and post-hoc multiple comparisons using the Holm-Sidak test ($\alpha = 0.01$). Number of analysed roots n = 10. Scale bars represent 10 µm; NLS = nuclear localisation signal.

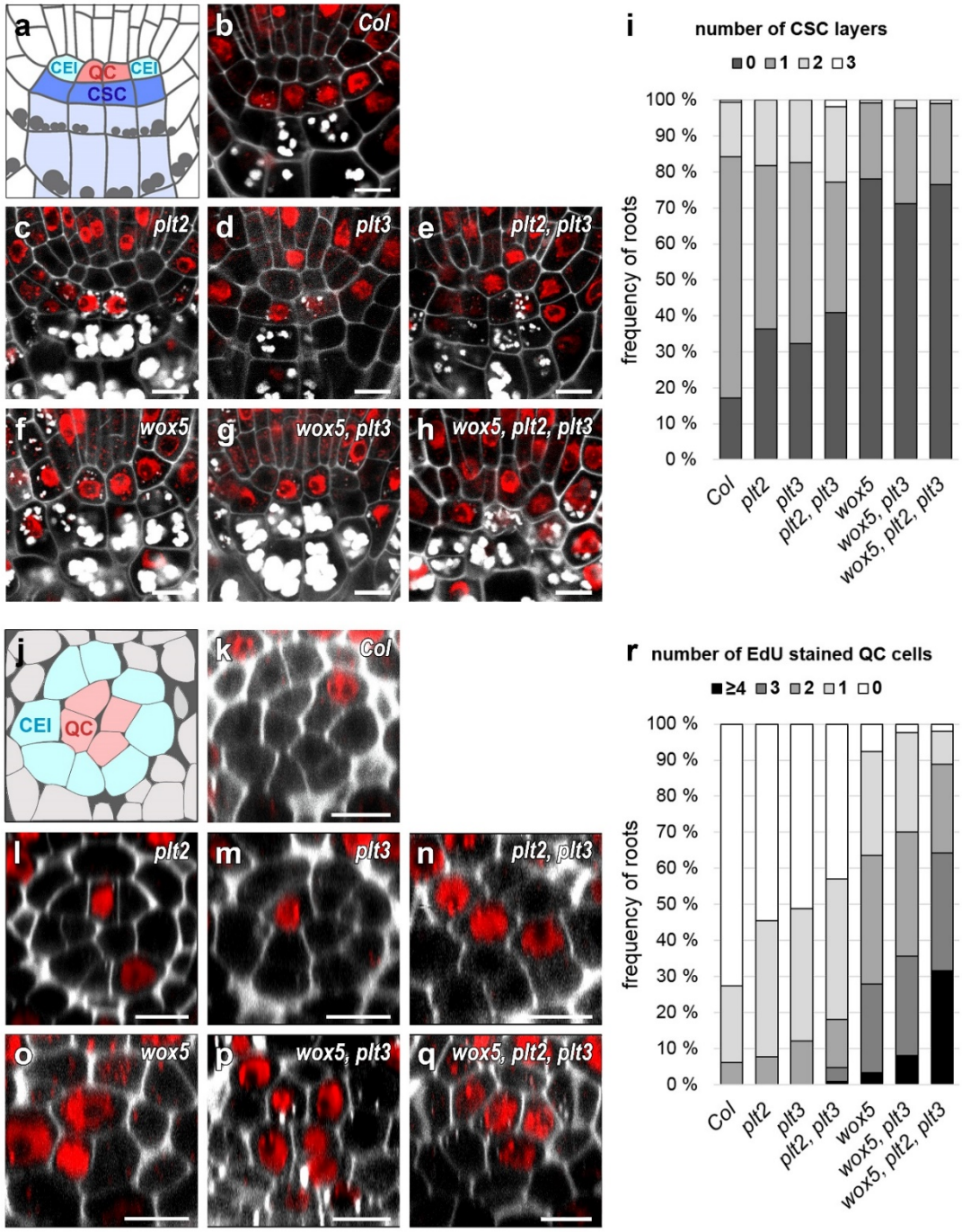

723 **Fig. 3 | *plt* and *wox5* mutants show more CSC differentiation and QC divisions. a**,
724 Schematic representation of a longitudinal section of an *Arabidopsis* RM. QC cells are marked
725 in red, CSCs are marked in dark blue, CCs in light blue. Combined mPSPI (grey) and EdU (red)
726 staining for 24 hours (SCN staining) in order to analyse the CSC (**a**-**i**) and QC division
727 phenotype (**j**-**r**) within the same roots. **b**-**h**, Representative images of the SCN staining in *Col*,
728 and the indicated single, double and triple mutant roots. **i**, Analyses of the SCN staining for

729 CSC phenotypes. Frequencies of roots showing 0, 1, 2, or 3 CSC layers are plotted as bar
730 graphs. **j**, Schematic representation of a transversal section of an *Arabidopsis* RM. QC cells are
731 marked in red, CEI initials are marked in turquoise. **r**, Analyses of the SCN staining for QC
732 division phenotypes. Frequencies of roots showing 0, 1, 2, 3 or ≥4 dividing QC cells are plotted
733 as bar graphs. Number of roots n = 77-146 from 2-5 independent experiments. QC = quiescent
734 center, CSC = columella stem cell, CEI = cortex endodermis initial, SCN = stem cell niche,
735 mPSPI = modified pseudo-Schiff propidium iodide, EdU = 5-ethynyl-2'-deoxyuridine, scale
736 bars represent 5 µm.

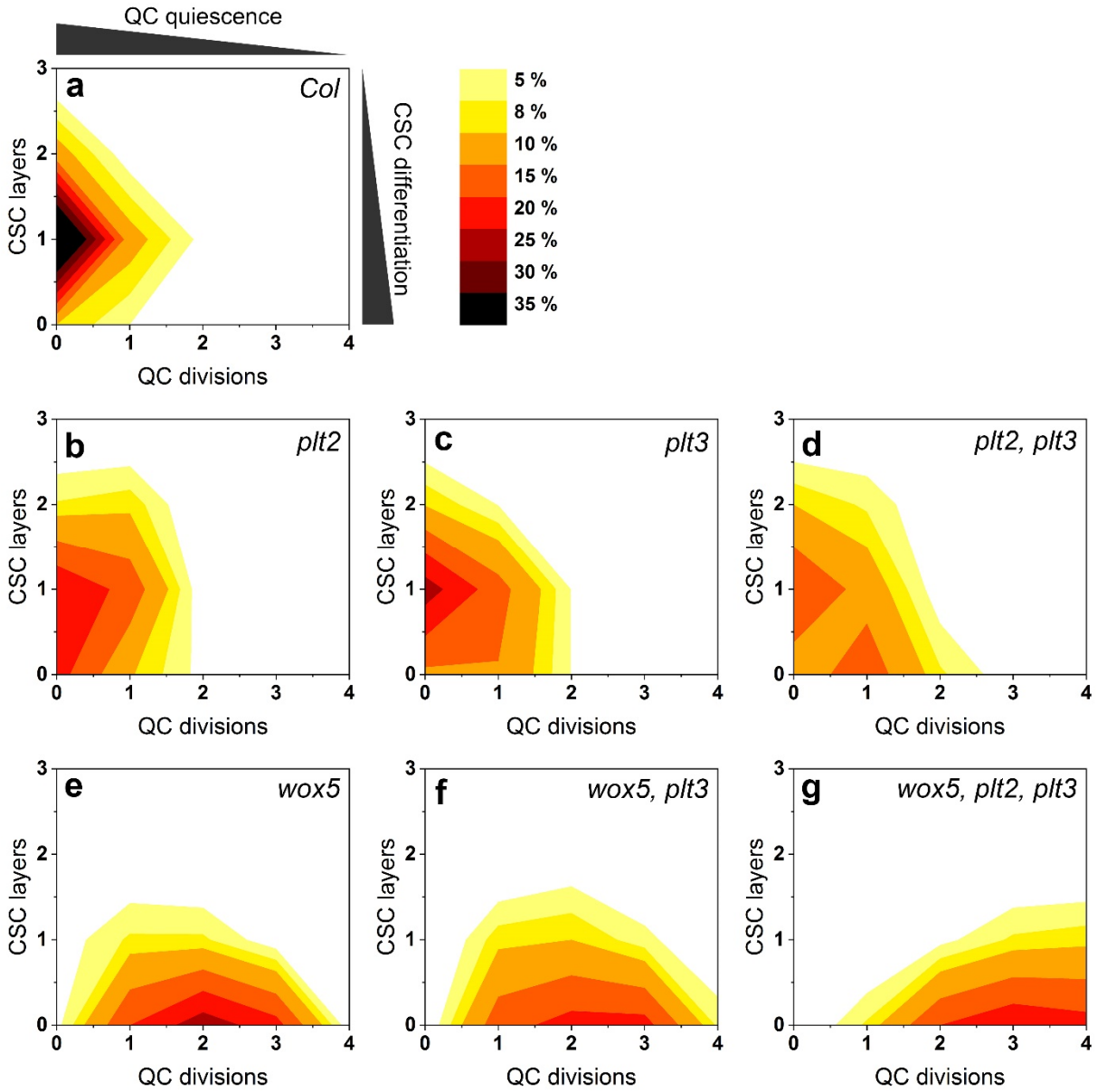

737 **Fig. 4 | QC divisions correlate negatively with the number of CSC layers.** The combined
738 results of the SCN staining in Fig. 3 are shown as 2D plots to visualise the correlation of the
739 CSC layer number and QC division. Number of CSC layers are shown on the y axis and the QC
740 division phenotype is shown on the x axis. The darker the colour, the more roots show the
741 respective phenotype (see colour gradient top right indicating the frequencies). *Col* wild type
742 roots show one layer of CSCs and no EdU stained cells (no QC division) after 24 h EdU
743 staining.

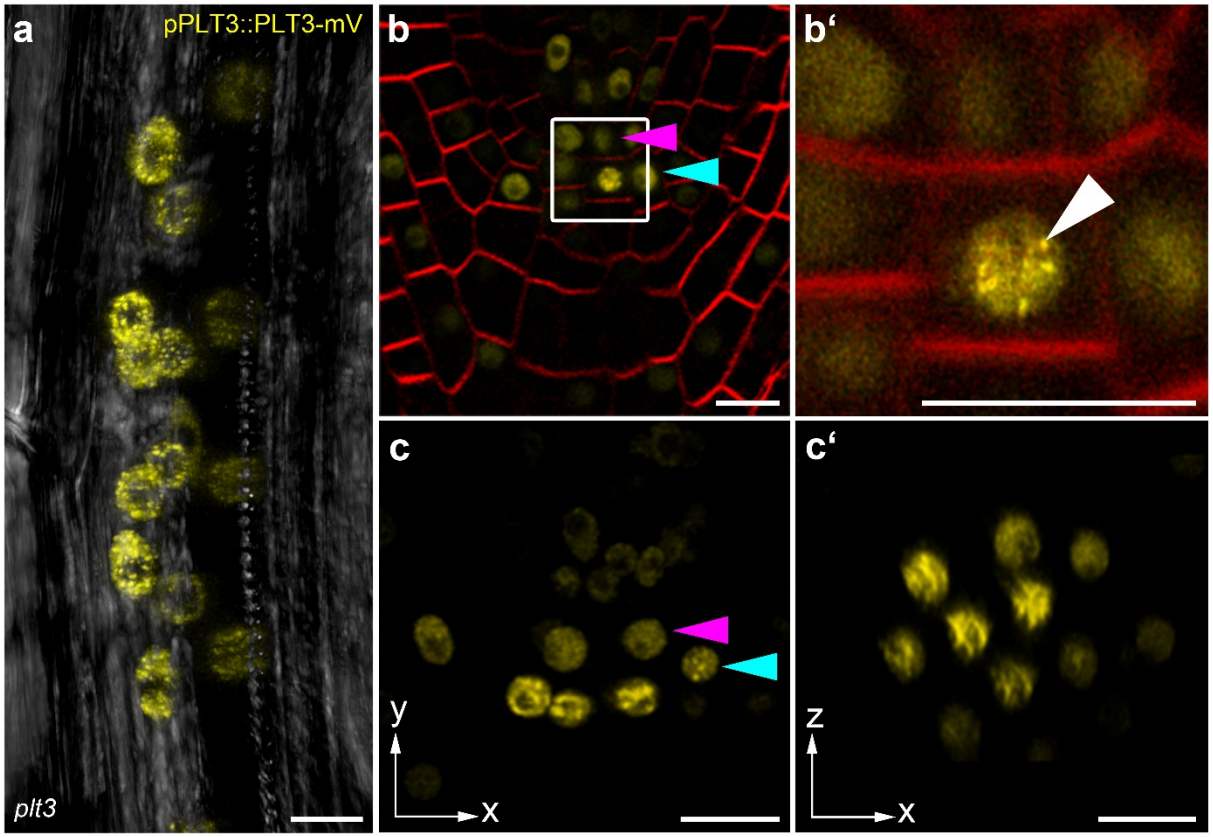

744 **Fig. 5 | PLT3 localises to NBs in *Arabidopsis thaliana* LRPs and CSCs. a-c’**, PLT3-mV
745 expression driven by the PLT3 endogenous promoter in LRP (**a**) and main root SCN (**b-c’**) in
746 *plt3* mutant *Arabidopsis* roots. **a**, representative image of PLT3-mV expression (yellow) in an
747 LRP showing the subnuclear localisation to NBs. Transmitted light image in grey. **b,b’**, SCN
748 of an PLT3-mV expressing FM4-64-stained (red) *Arabidopsis* main root. The magnification of
749 the CSC layer (**b’**) shows the subnuclear localisation of PLT3 to NBs in a CSC. White
750 arrowhead points at a NB. **c,c’**, SCN of an PLT3-mV expressing *Arabidopsis* main root. NBs
751 are visible in the CSC layer in **c**, also in the transversal view of the CSC layer (**c’**). Arrowheads
752 in **b** and **c** point at the QC (magenta) and CSC (cyan) positions. mV = mVenus; LRP = lateral
753 root primordium; SCN = stem cell niche; NBs = nuclear bodies; CSC = columella stem cell.
754 Scale bars represent 10 µm.

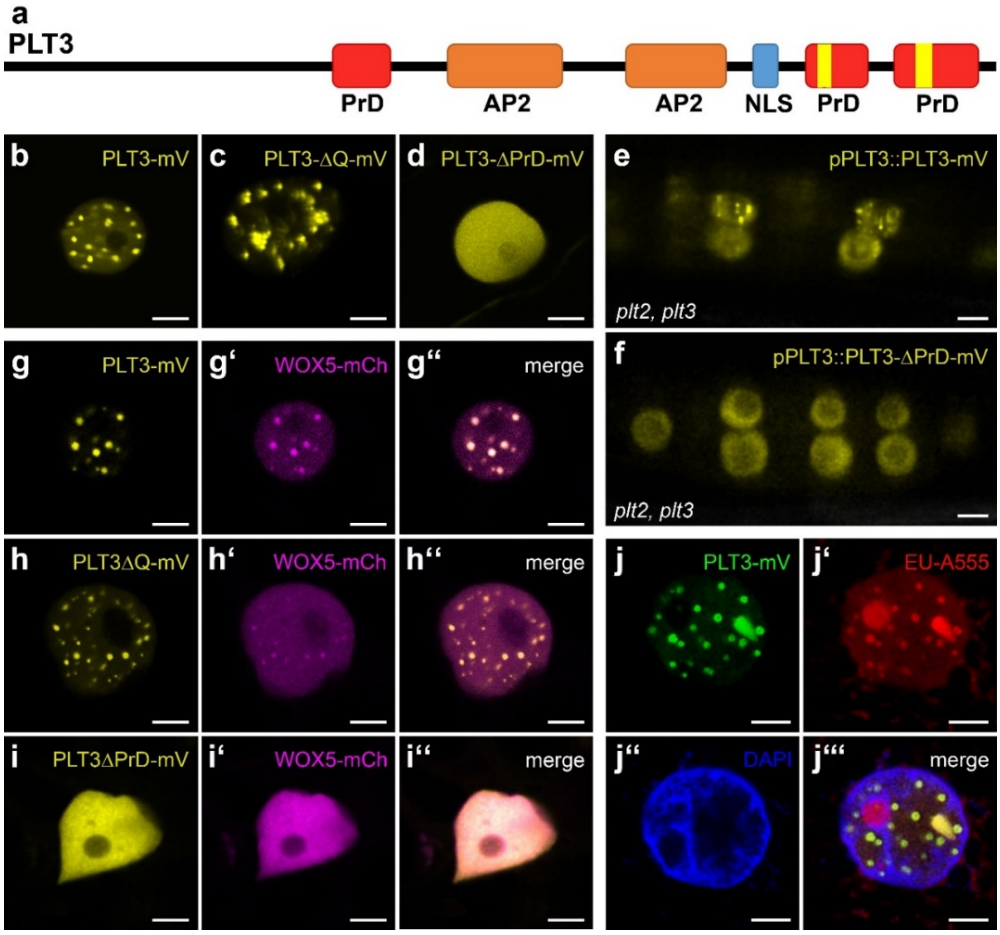

Fig. 6 | PLT3 PrD domains influence its subnuclear localisation. a, schematic representation of PLT3 protein domains. The areas in red are predicted prion-like domains (PrDs) and were deleted in PLT3-ΔPrD-mV. The areas highlighted in yellow contain polyQ-stretches and were deleted in PLT3-ΔQ-mV. **b-d** Expression of PLT3-mV (**b**), PLT3-ΔQ-mV (**c**) and PLT3-ΔPrD-mV (**d**) in transiently expressing *N. benthamiana* leaf epidermal cells. **e**,**f**, PLT3-mV (**e**) and PLT3-ΔPrD-mV (**f**) expression driven by the PLT3 endogenous promoter in lateral root primordia of *plt2, plt3* double mutant *Arabidopsis* roots. **g-i’’**, Co-expression of PLT3-mV (**g**), PLTΔQ-mV (**h**) and PLT3ΔPrD-mV (**i**) with WOX5-mCh (**g’,h’,i’**) in transiently expressing *N. benthamiana* leaf epidermal cells. **j-j’’’**, Expression of PLT3-mV (**j**) in transiently expressing *N. benthamiana* leaf epidermal cells in combination with RNA staining with EU (18 h), visualised by click-reaction with Alexa Fluor® 555 (**j’**) and a DNA staining with DAPI (**j’’**). mV = mVenus; PrD = prion-like domain; AP2 = APETALA2 domain; NLS = nuclear localisation signal; EU = 5-ethynyl-2’-uridine. Scale bars in (**b-j’’’**) represent 5 µm.

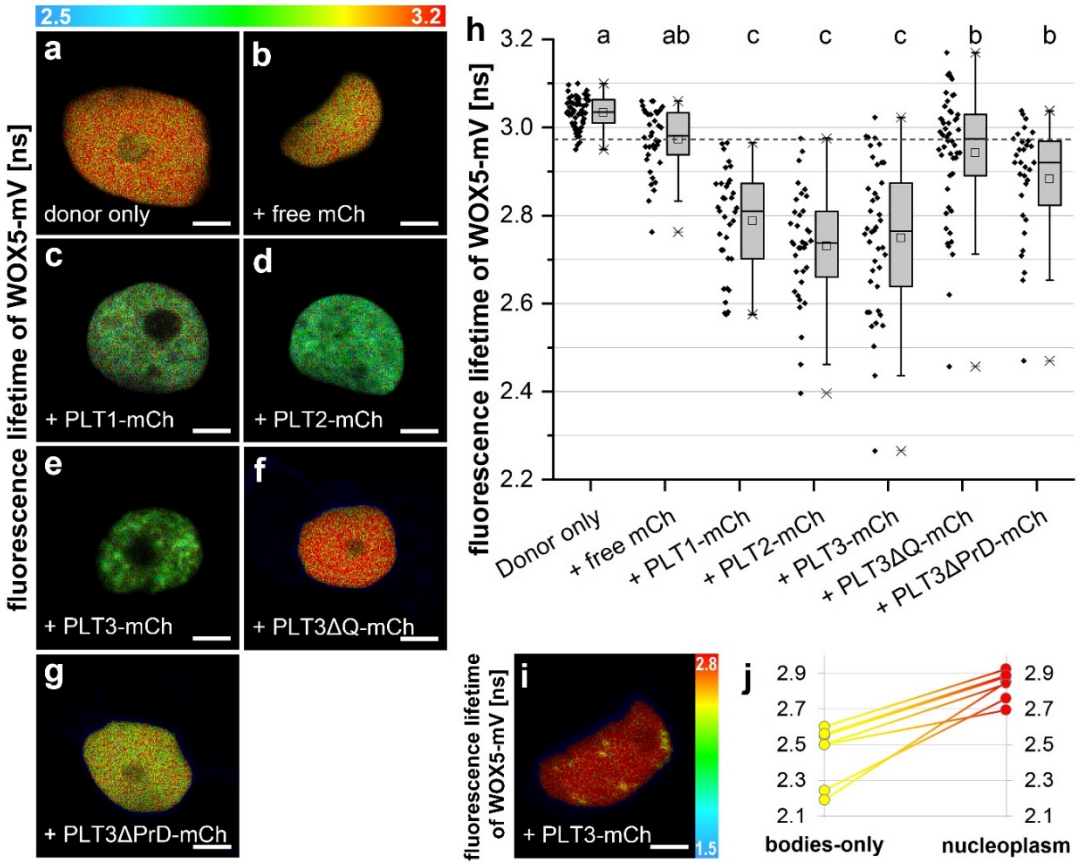

768 **Fig. 7** | **WOX5 can interact with PLTs. a-h**, Fluorescence Lifetime Imaging (FLIM) results
769 of transiently expressing *N. benthamiana* leaf epidermal cells. **a-g,i** FLIM images of WOX5-
770 mVenus (donor only) plus the indicated acceptors after a pixel-wise mono-exponential fit of
771 the mVenus fluorescence signal. The fluorescence lifetime of WOX5-mVenus in ns is color-
772 coded. Low lifetimes (blue) due to FRET indicate strong interaction of the two proteins and
773 high lifetimes (red) indicate weaker or no interaction. Scale bars represent 5 µm. **h**,
774 Fluorescence lifetimes in ns are summarized in combined scatter and box plots. Statistical
775 analysis of samples was carried out by one-way ANOVA and post-hoc multiple comparisons
776 using the Holm-Sidak test. Samples with identical letters do not show significant differences
777 ($\alpha = 0.01$; $n \geq 32$). Box = 25-75 % of percentile, whisker = 1.5 interquartile range, – = median,
778 □ = mean value, × = minimum/maximum. **j**, 7 individual nuclei showing nuclear bodies during
779 co-expression of WOX5-mV and PLT3-mCh were analysed for WOX5-mV lifetime in the
780 nuclear bodies or nucleoplasm separately. mCh = mCherry. mV = mVenus.

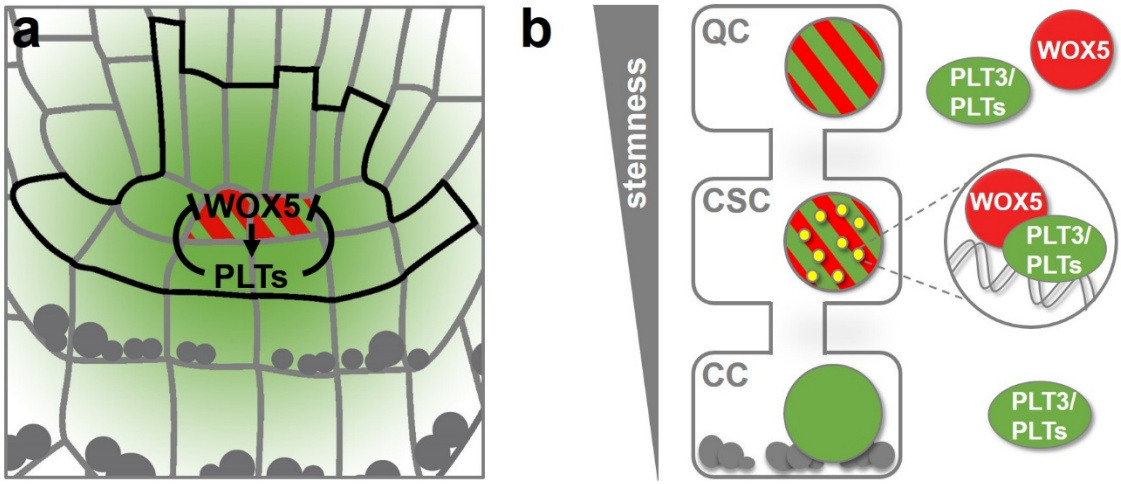

781 **Fig. 8 | Model of PLT and WOX5 transcriptional regulation, interaction and subnuclear**
782 **localisation during distal root stem cell maintenance.**

783 **a**, Transcriptional regulation of *WOX5* (red) and *PLT* (green) expression by negative feedback
784 regulation in the *Arabidopsis* RAM. *WOX5* is expressed in the QC and promotes *PLT*
785 expression, whereas *PLT* expression is restricting the *WOX5* expression domain to the QC
786 position. **b**, Both WOX5 (red) and PLT3 (green) are present homogenously within the nuclei
787 of the QC cells. WOX5 can move to the CSCs and is recruited there by PLT3 to NBs (yellow),
788 where interaction takes place. This maintains the stem cell character of the CSCs but already
789 leads to a determination to subsequent CC fate.